PHYSICAL REVIEW B VOLUME 35, NUMBER 6 15 FEBRUARY 1987-II

Near-edge x-ray-absorption fine structure in uranium compounds

G. Kalkowski, G. Kaindl, W. D. Brewer, and W. Krone
Institut für Atom- und Festkörperphysik, Freie Universität Berlin, Arnimallee 14, D-1000 Berlin 33, Germany

(Received 25 August 1986; revised manuscript received 9 December 1986)

For a number of metallic and nonmetallic U systems as well as a few Th compounds, the near-edge x-ray-absorption fine-structure spectra, taken by transmission and total-electron-yield techniques, are reported at the L_3, M_3, $M_{4,5}$, $N_{4,5}$, and $O_{4,5}$, thresholds. At L_3 and M_3, similar spectra with analogous information are observed. While in the metallic U systems, the white lines at L_3 and M_3 show only minor variations in position and relative peak height, a shift of $\simeq 4$ eV is observed between UCl_3 and UF_4, representing mainly the difference in Coulomb interaction between a $2p_{3/2}$ core hole and the $5f$ configurations. The spectra at the $M_{4,5}$ and $N_{4,5}$ thresholds are dominated by intense absorption peaks due to $3d$-$5f$ and $4d$-$5f$ transitions probing directly the unoccupied $5f$ states. No multiplet structure due to $3d$-$5f$ or $4d$-$5f$ exchange interaction is resolved, but the linewidths of the $M_{4,5}$ peaks in the metallic U systems are found to decrease by $\simeq 20\%$ with increasing U-U distance, reflecting a narrowing of the unoccupied $5f$ bands. The spectra at the $O_{4,5}$ thresholds, on the other hand, show well-resolved structures, which are atomiclike for ThF_4 and UF_4 and may be described by spin-orbit and exchange splitting of the $5d^9 5f^1$ and $5d^9 5f^3$ final states, respectively. In metallic U systems, the $O_{4,5}$ structures are broadened and partly lost, presumably due to the more itinerant nature of the $5f$ states. Additional relatively weak peaks are observed in the $M_{4,5}$ and $O_{4,5}$ spectra of Th metal, ThO_2, UO_2, and UF_4 at energies from $\simeq 15$ to 38 eV above threshold, which are assigned to multiple-scattering resonances.

I. INTRODUCTION

The electronic structure of light actinide (A) compounds is dominated by the $5f$ electrons, which are on the borderline between localized and itinerant electronic behavior. It is well known that the $5f$ electrons are less localized than the rare-earth (RE) $4f$ states, but not as itinerant as the transition-metal $3d$ electrons. In addition, profound changes from itinerant to localized $5f$ behavior are known to occur when going across the actinide series. The electronic properties of actinide compounds have often been compared with those of the light RE elements, particularly of cerium, although the transition to localized $5f$ behavior proceeds far more gradually in the actinide series, reaching from U to Am. In this intermediate region, strong differences in $5f$ localization occur in different compounds as well as under the influence of external pressure.[1,2] Such differences in $5f$ localization are known for U systems: Photoemission (PE) and bremsstrahlung isochromat spectroscopy (BIS) studies, e.g., characterize α-U metal as a rather itinerant $5f$ system,[3] while UPd_3,[4] UTe,[5] and particularly UO_2,[6] are more localized.

This situation stimulates the strong present interest in experimental information on the electronic structure of actinide compounds. However, due to the radioactivity of the actinide elements, an increasing number of theoretical calculations on the electronic structure is not matched by experimental results. The radioactivity problems are particularly prohibitive in photoemission studies using synchrotron radiation, but also in bremsstrahlung isochromat spectroscopy studies,[3] since in both spectroscopies bare radioactive samples with clean surfaces are used. Information on the electronic structure, though less direct, may also be obtained from near-edge x-ray-absorption fine-structure (NEXAFS) spectra.[7-9] At x-ray-absorption (XA) thresholds with energies above $\simeq 3$ keV, encapsulated samples may be used, greatly simplifying the problem of handling these highly radioactive materials.

With future applications of XA techniques to compounds of Np, Pu, Am, and of the heavier actinide elements in mind, we have therefore undertaken an exploratory study of NEXAFS spectra of a number of metallic and insulating U systems and—for comparison—also of a few Th compounds. The absorption spectra were recorded with the use of synchrotron radiation at a variety of XA thresholds spanning the energy range from 110 eV ($O_{4,5}$ thresholds) to 17.2 keV (L_3 threshold). Both the standard transmission technique (at L_3, M_3) and the total-electron-yield method (at M_3, $M_{4,5}$, $N_{4,5}$, and $O_{4,5}$) were employed.

Up to now, XA studies of U and heavier actinide compounds have been very scarce. Previous work includes early $M_{4,5}$ XA spectra of α-U metal, UO_2, and Pu metal,[10-12] as well as a study of the $O_{4,5}$ thresholds of α-U metal and gas-phase UF_4.[13] More recently, NEXAFS spectra have been reported for a few intermetallic compounds of U at the L_3 and $M_{4,5}$ thresholds,[14] and polarization-dependent L_1 and L_3 spectra were measured for a single crystal of rubidium uranyl nitrate.[15] During the course of this study, a parallel investigation of L_3 and $M_{4,5}$ NEXAFS spectra of uranium oxides and glasses came to our attention.[16]

In general, NEXAFS spectra may be quite complex, since both single-particle transitions and many-body phenomena, as well as lifetime broadening, phonon interaction, and other factors may contribute.[7,8] In systems with a high density of unoccupied states, the XA spectra at those thresholds which couple optically to these states are dominated by an intense peak (white line). In a single-particle picture using Fermi's golden rule, the line shape of such a white line is given by the partial density of unoccupied states with the optically allowed angular momentum. Such strong white-line resonances are well known for the $L_{2,3}$ XA edges of $3d$ transition elements[9,17] and RE compounds,[18] as well as for the $M_{4,5}$ and $N_{4,5}$ spectra of RE systems.[19–23] They probe the partial unoccupied density of states with a resolution given by the core-hole lifetime width and the instrumental resolution. The influence of the core hole may also lead to configuration-interaction effects in the final state, which have been identified in L_3-edge spectra of RE compounds[24] and theoretically treated for a number of core-level spectroscopies.[25,26] In situations with highly localized final states, e.g., at the $M_{4,5}$ thresholds of RE compounds, the NEXAFS spectra may be governed by characteristic multiplet structures from the exchange interaction between the core hole and the open final-state shell.[20–22]

In addition to these transitions probing the unoccupied electronic structure, NEXAFS peaks due to multiple scattering (MS) of photoelectrons between neighboring atoms and the atom under study are frequently observed. These MS NEXAFS resonances probe the spatial arrangement of neighboring atoms, and they are known to be strong in XA spectra of chemisorbed molecules.[27] They are also frequently encountered in bulk solids, particularly in those with a well-defined and highly coordinated nearest-neighbor shell.

The present paper is organized as follows. After a brief description of the experimental procedure in Sec. II, an overview of the NEXAFS spectra at the five investigated threshold regions is given in Secs. III to VII; Sec. VIII finally contains a summary and the conclusions of the present work.

II. EXPERIMENTAL DETAILS

The intermetallic compounds studied in this work were arc melted from the constituent elements of at least 99.9% purity. UO_2 was available as a single crystal, while the other nonmetallic compounds of high purity were polycrystalline powders from commercial suppliers. All compounds were analyzed by the Debye-Scherrer method with the result that no impurity phases were detected except in UO_3; this compound was found to be mainly γ-UO_3,[28] with minor traces of other oxide phases.

The L_3-edge data were taken at the ROEMO beam line of HASYLAB, DESY, employing a pair of Si(311) crystals. The resolution of the spectrometer was $\simeq 5$ eV [full width at half maximum (FWHM)] at the $2p_{3/2}$ threshold of U, and all L_3-edge data were taken in transmission geometry. Three ionization chambers mounted in series allowed us to measure simultaneously the absorption of the sample under study and that of a reference material, in order to accurately determine relative shifts in edge position. Typical absorber thicknesses were 12 mg/cm^2 for the insulating U compounds and 25 mg/cm^2 for the metallic systems. The latter were prepared by filing the material under Ar atmosphere and mixing the fine powder with wax; the sample was then sealed in a lucite capsule and stored under Ar. Some nonmetallic U compounds were also investigated in the regions of the M_3 and M_5 edges in transmission geometry, using the same setup to determine relative energy shifts for the M_3 edges. These studies were performed at the EXAFS-II beam line of HASYLAB employing Si(111) crystals; in this case the resolution was $\simeq 1.7$ eV (FWHM).

Additional M_3- and $M_{4,5}$-edge measurements on metallic as well as nonmetallic U compounds were performed at the JUMBO monochromator of Stanford Synchrotron Radiation Laboratory (SSRL), Stanford during parasitic conditions. Using Ge(111) crystals, energy resolutions of 1.4 eV at the Th M_5 edge and 1.8 eV at the U M_3 edge were obtained, determined from the rocking curves. For deconvolution purposes, rocking curves were measured at a number of photon energies between 3.2 and 4.5 keV after several injections in order to account for different beam conditions. The energy calibration of JUMBO was adjusted to 3330 eV for the Pd L_2 edge and to 4302 eV for the U M_3 edge and found to be reproducible within 0.5 eV. Normalization of the total-electron-yield spectra to photon flux was found essential and was achieved by monitoring the total electron yield from a nickel grid at the monochromator exit.

The $N_{4,5}$- and $O_{4,5}$-edge data were taken at the SX-700 beam line of BESSY, Berlin with resolutions of 1.4 and 0.1 eV, respectively. In order to achieve high resolution at the $N_{4,5}$ thresholds, the monochromator was operated when electron currents less than 30 mA were in the storage ring; this guaranteed small emittance of BESSY. Additionally, the acceptance angles of both the monochromator and the ellipsoidal focusing mirror were reduced. The resolution at the $N_{4,5}$ thresholds of U was determined from a study of the M_5 XA spectrum of LaF_3.[20] The $N_{4,5}$ measurements reported were performed in a total-electron-yield mode during a single injection in order to minimize energy shifts due to changes in source position.

For the total-electron-yield measurements, the surfaces of the metallic compounds and of UO_2 were cleaned *in situ* by scraping with a diamond file at a base pressure of 10^{-10} torr. The other oxides and fluorides were painted as alcohol-based suspensions on Ta or Al substrates before being transferred into the ultrahigh vacuum (UHV) system. Typical data acquisition times were 30 min for a complete $M_{4,5}$ scan and 15 min for the other spectra.

III. OVERVIEW OF XA SPECTRA FOR UF_4

An overview of the NEXAFS spectra of UF_4 obtained at the various thresholds investigated is given in Fig. 1; the spectra are plotted on a common relative energy scale with the experimental resolution ΔE (FWHM) specified in each case. In the upper part of the figure, the absorption coefficient as obtained from transmission measurements (in arbitrary units) is plotted versus the photon energy. The spectra in the lower part of the figure were obtained by monitoring the total electron yield from the sample surface as a function of photon energy and normalizing it to the incoming photon flux. This normalized yield signal is proportional to the absorption coefficient to a good approximation.

The upper two curves in Fig. 1 represent the photon absorption at the L_3 and M_3 thresholds due to optical transitions from $2p_{3/2}$ and $3p_{3/2}$ core levels, respectively, into unoccupied states. The peaks at the onset of the edges (white lines) correspond to transitions into unoccupied states with $6d$ symmetry, while the underlying edge structure stems from transitions into the continuum; above threshold, structures due to multiple scattering of the outgoing photoelectrons are visible. The L_3 and M_3 spectra look quite similar, as expected from the analogous final states, which differ only by the presence of a $2p_{3/2}$ and $3p_{3/2}$ core hole, respectively. Note that in the present study the experimental resolution at M_3 is better by a factor of $\simeq 2.5$ compared to L_3, mainly due to the lower photon energy.

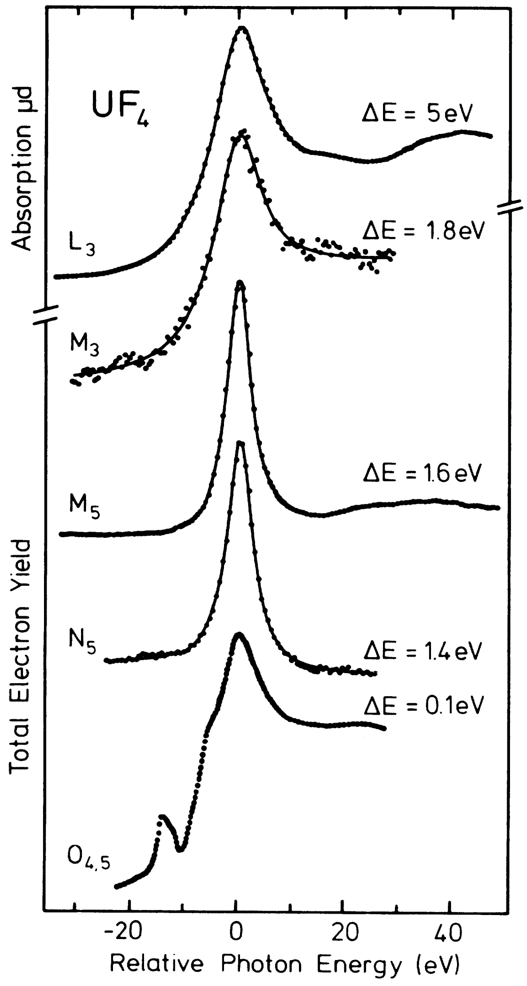

FIG. 1. Near-edge XA fine-structure spectra of UF$_4$ at the L_3, M_3, M_5, N_5, and $O_{4,5}$ thresholds, which are located at photon energies of about 17 180, 4310, 3550, 730, and 110 eV, respectively. For each spectrum the energy resolution ΔE (FWHM) of the employed monochromator is given.

Also shown in Fig. 1 are the NEXAFS spectra of UF$_4$ at the M_5 and N_5 thresholds, corresponding to transitions from $3d_{5/2}$ and $4d_{5/2}$ core levels, respectively, into unoccupied states of mainly $5f$ symmetry. In both cases, intense white lines are observed, with only a very weak edge jump at the M_5 threshold and practically none at N_5. In the white-line peaks at both the M_5 and N_5 thresholds, no multiplet structure due to exchange interaction between the core hole and the open $5f$ shell is resolved. The analogous M_5 and N_5 spectra of the RE elements, on the other hand, are characterized by well-resolved multiplet splittings.[19–23] These differences are readily explained by the much smaller overlap of the $3d$ and $4d$ core-hole wave functions with the U $5f$ states as compared to the RE $4f$ states. The relatively weak edge jump observed at the M_5 threshold is due to transitions into mf and np states of the continuum (with $m \geq 6$ and $n \geq 7$). These transitions are relatively more intense in the light actinide spectra than in the RE $M_{4,5}$ spectra, both since the centrifugal barrier is lower and since the $3d$-$5f$ transition matrix element is reduced in comparison to $3d$-$4f$.[29] The absence of an observable edge jump at N_5 is presumably caused by the high oscillator strength for transitions into $5f$ states due to the large $4d$-$5f$ orbital overlap.

Finally, Fig. 1 also contains the photoabsorption spectrum in the $O_{4,5}$-threshold region of UF$_4$. In contrast to the M_5 and N_5 spectra, a complex near-edge structure is observed, indicating $5d^9 5f^{n+1}$ multiplet splitting; this is analogous to the situation at the $N_{4,5}$ thresholds of the RE elements.[23,30] In the latter cases, the exchange interaction between a $4d$ hole and the $4f^{n+1}$ configuration exceeds the spin-orbit coupling, leading to a spectrum which is no longer given by separate $4d_{5/2}$ (N_5) and $4d_{3/2}$ (N_4) contributions. As discussed in more detail below, this is similar to the $O_{4,5}$ spectra of Th and U systems.

IV. NEAR-EDGE FINE STRUCTURE AT THE L_3 AND M_3 THRESHOLDS

A detailed comparison of the L_3 edge shapes of various U systems is presented in Fig. 2. These spectra were all recorded against a reference sample of UF$_4$, so that the relative energy scale is accurate to ±0.2 eV, allowing a comparison of the energies of the white-line peaks. The spectra reflect considerable variations in width and relative amplitude of the white-line peaks. In particular, the white-line amplitude decreases when proceeding from ionic UF$_4$ or UO$_2$ to the intermetallic systems UCu$_5$ and UNi$_5$, and further to α-U metal. Also, small shifts to lower energy relative to UF$_4$ occur for the white lines in the metals, while $\simeq$2-eV shifts to higher energy are observed for UO$_3$ and U$_3$O$_8$. Note a pronounced shift in the white-line position by 4.1 eV to lower energy in trivalent UCl$_3$ as compared to tetravalent UF$_4$. This is essentially the difference in Coulomb interaction, $U_{2p\text{-}5f}$, between the $2p_{3/2}$ core hole and the $5f$ electronic states of the two compounds and demonstrates the screening power of an additional $5f$ electron. Even though no theoretical estimates are presently available for $U_{2p\text{-}5f}$, the experimental result is quite reasonable in comparison with the known values for $U_{2p\text{-}4f}$ in rare-earth systems.[31]

Also striking are changes in line shape of the white-line peaks in the L_3 spectra of Fig. 2. While the white lines observed for UF_4 and UCl_3 are intense and relatively narrow, a strong variation in the white-line amplitude relative to the edge jump is observed in the metallic systems. These changes mainly reflect variations in the unoccupied $6d$ density of states from UF_4 to α-U metal, with a relatively large $6d$ bandwidth for the latter. Such a correlation between the L_3 white lines and ground-state densities of unoccupied states has been shown to hold for rare-earth metals.[18]

The white line of UNi_5 is shifted by $\simeq 2$ eV relative to that of UCu_5, and it is also rather asymmetric. This difference is interesting in view of the peculiarities reported in lattice constant, susceptibility, and specific heat for the $UNi_{5-x}Cu_x$ series of compounds.[32] Recently, BIS measurements on this system indicated that the $5f$ states are rather itinerant in UNi_5 and more localized in UCu_5.[33] This suggests that the variations in the L_3 white lines are caused by variations in the $6d$ density of states (DOS) due to $5f$-$6d$ hybridization.

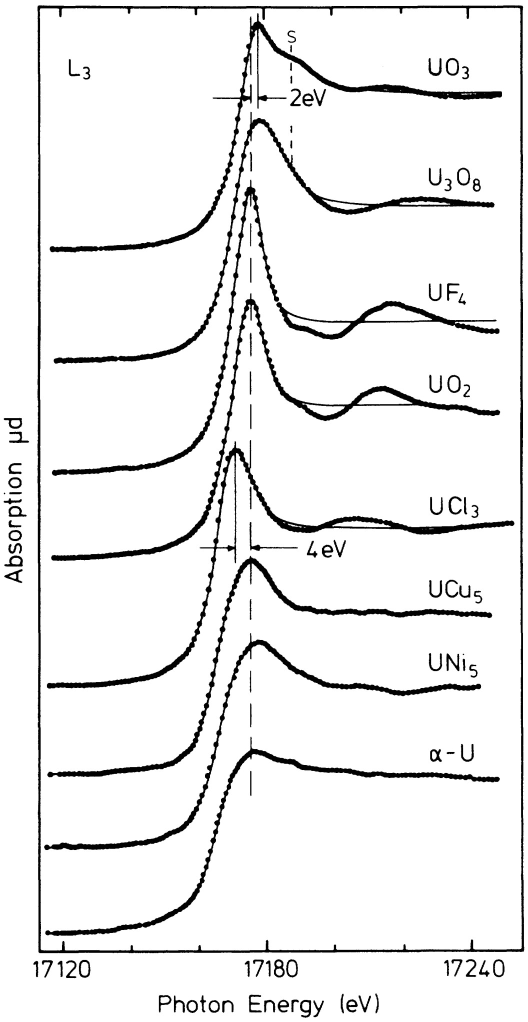

FIG. 2. Near-edge XA fine-structure spectra at the L_3 thresholds of various U compounds. The solid lines represent the results of least-squares fits as described in the text.

In the spectrum of UO_3, a second peak (S) is observed, shifted by $\simeq 9$ eV to higher energies; it is broader than the main white-line peak and its intensity amounts to $\simeq 80\%$ of the latter. A similar high-energy shoulder may cause the asymmetric broadening of the white line in U_3O_8, but additional complexity arises in this compound due to the presence of formally pentavalent as well as hexavalent U sites. Such double-peaked white lines are well known from the L_3 spectra of mixed-valent RE systems.[24,31,34] In the present case, however, an interpretation along these lines appears less promising, since the 9-eV splitting cannot easily be reconciled with the shift value of $\simeq 4$ eV for $U_{2p\text{-}5f}$ determined in this work. On the other hand, a considerable amount of covalent $5f$ character must be expected for hexavalent U compounds, as borne out in the results of a band-structure calculation for UF_6.[35] This would support an interpretation of peak S in terms of a core-hole—induced many-body effect, in analogy to the L_3-edge spectra of CeF_4 and CeO_2. Note that comparable features were found previously in the XA spectra of $3d$ compounds in parallel to the occurrence of satellite peaks in core-level PE;[36] such PE satellites are characteristic for

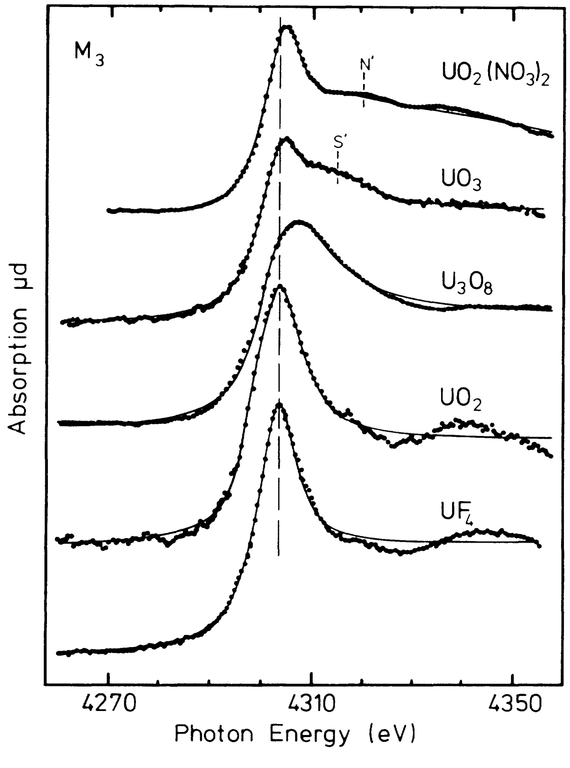

FIG. 3. Near-edge XA fine-structure spectra of some nonmetallic U compounds at the M_3 threshold. The solid lines represent fit results.

all the U oxides under study, and are particularly intense for UO_3.[37]

Alternatively, an interpretation is possible in terms of a MS resonance previously identified in the L_1- and L_3-edge spectra of rubidium uranyl nitrate.[15,16] Using a single crystal of rubidium uranyl nitrate and making use of the linearly polarized nature of synchrotron radiation, it is shown in this work that a peak $\simeq$15 eV above the main white line is due to multiple scattering of the photoelectron in the linear O—U—O uranyl bond. Since the energy E (relative to threshold) of a MS resonance depends on the interatomic distance r to a first approximation as $E \propto r^{-2}$ (neglecting the energy dependence of the phase shifts), an increased U—O separation in UO_3 as compared to that of the uranyl group would be expected. This is indeed the case, even though the quantitative agreement is not very good. The spectra in Fig. 2 were analyzed by fitting a Lorentzian to the white line and an arctangent function to the edge jump, convoluted with a Gaussian of 5 eV (FWHM) to account for experimental resolution. This procedure corresponds to standard L_3-edge analysis in the case of RE systems;[31] in the absence of detailed edge-shape calculations, it may be used to deduce variations in bonding from the positions and widths of the Lorentzians. We prefer this approach rather than a determination of the edge position from the point of inflection, since linewidth effects can be distinguished from shifts in the white-line position. In the case of α-U, UNi_5, and U_3O_8, no reasonable fits were obtained with this simple model; an asymmetric Lorentzian line shape had to be introduced for a proper description of the white lines.[38] The results of these fits are summarized in Table I and indicated by solid lines in Fig. 2.

In order to gain more insight into the near-edge spectra of UO_3 and U_3O_8, we have also investigated the photon absorption spectra at the $3p_{3/2}$ thresholds (M_3 edges), with better instrumental resolution. The spectra obtained are presented in Fig. 3. Consistent with the L_3-edge results, a second peak (S') is found $\simeq$9.5 eV above the white line in UO_3, which is much broader (by a factor of 2.5) than the main peak. The white line is shifted by $\simeq$1.6 eV to higher energy relative to UO_2 and by $\simeq$2 eV to lower energy with respect to U_3O_8. Hexavalent $UO_2(NO_3)_2 \cdot 6H_2O$ [designated $UO_2(NO_3)_2$ in Fig. 3] shows a similar shift in line position to UO_3,[39] but no comparable satellite feature 9 eV above the edge. Instead, a MS peak (N'), separated by $\simeq$15 eV from the white line, is observed in agreement with the observations of Ref. 15. For U_3O_8, a single broad feature is observed, which can be fitted by a single asymmetric line. Due to the absence of structure, no attempt was made to decompose the spectrum into separate components.

We have also studied the M_3 edges of a series of metallic U systems employing the total-electron-yield method and using bulk samples in ultrahigh vacuum. This excludes the possibility of measuring the sample under study simultaneously with a reference compound for energy calibration purposes. By comparing different runs for the same compound, however, we find the results to be reproducible within ± 0.3 eV. From a recent total-electron-yield study of the Tm $M_{4,5}$ thresholds at $\simeq$1500 eV,[20] we estimate the sampling depth at the present energies to be $\simeq$100 Å, i.e., much smaller than the penetration depth of the x rays. The resulting spectra are presented in Fig. 4. Comparing the data for UF_4 and UO_2 with those obtained in the absorption measurements (see Fig. 3), we notice that

TABLE I. Parameters from fits of the L_3- and M_3-edge spectra by a Lorentzian for the "white line" plus an arctangent function for the "edge jump." δ gives the energy shift of the white line relative to UF_4 and ThF_4 for the uranium and thorium compounds, respectively; W represents the width of the white line (FWHM), deconvoluted with the experimental resolution [to account for experimental resolution, the Lorentzian, and arctangent function were convoluted with Gaussians of total width (FWHM) 5 eV (U L_3), 4.8 eV (Th L_3), and 1.8 eV (U M_3), respectively]; α indicates the asymmetry parameter (see text).

	L_3 edge (transmission)			M_3 edge (transmission)			M_3 edge (total electron yield)	
	δ (eV)	W (eV)	α	δ (eV)	W (eV)	α	δ (eV)	W (eV)
$UO_2(NO_3)_2 \cdot 6H_2O$	+1	9		+1.3	10			
UO_3	+2	9		+1.6	7.8			
	+10	17		+11	19			
U_3O_8	+3	12	1.3	+3.5	16	1.3		
UF_4		8			8.5			9.2
UO_2	0	9		+0.1	10		−0.1	10
α-U	−1	21	1.5				−0.2	17
UPt	−2	15					−0.5	16
UNi_5	+2	17	1.2				+2.5	14
UCu_5	0	12					−0.2	12
UPt_5	−1	14					−0.4	13
UCl_3	−4	11						
ThF_4		6						
ThO_2	0	7						
Th	−2	13						12

the two techniques, total electron yield and absorption, lead to essentially identical results. While the statistical accuracy of the total-electron-yield spectra presented is relatively poor due to unfavorable experimental conditions ("parasitic" mode at SSRL, with only $\simeq 5$ mA stored electron current at 1.5 GeV energy), and details are not well resolved, these measurements nevertheless demonstrate the potential of this spectroscopy. Since the samples were freshly filed in UHV, effects due to surface oxidation may be excluded, and the usual problems of transmission experiments (due to saturation and limited homogeneity of the absorbers) are absent.[40]

We summarize the results of the L_3 and M_3 experiments as follows: The chemical shifts between tetravalent and hexavalent U compounds are found to be rather small, amounting to no more than 2 eV, in contrast to the 4-eV shift between tetravalent and trivalent U compounds. This trend corroborates the idea of relatively extended $5f$ states in U compounds of valencies higher than four, and a correspondingly increased $5f$ localization in trivalent nonmetallic U systems. The similarity in shape of the L_3- and M_3-edge spectra is expected on the basis of the extended nature of the $6d$ final states and the localized nature of the $2p_{3/2}$ and $3p_{3/2}$ core holes. In fact, a slightly larger difference in linewidth between the L_3 and M_3 white lines of UF_4 or UO_2 would be expected from the lifetimes of the $2p_{3/2}$ and $3p_{3/2}$ core holes, which were calculated to be $\simeq 8$ eV and $\simeq 12$ eV, respectively.[41] Such differences are not observed in the spectra, and these numbers seem to be slightly overestimated in view of the experimental white-line widths given in Table I, which also contain the $6d$ bandwidths. In comparison to previous L_3-edge measurements on metallic U systems,[14] we find close agreement with the white-line shapes and widths, except for U metal, where our analysis gives a somewhat broader white line; this is also reproduced in the total-electron-yield spectra taken at the M_3 thresholds.

V. $3d$-$5f$ RESONANCES AT THE $M_{4,5}$ THRESHOLDS

Transitions from the $M_{4,5}$ subshells into unoccupied states of mainly $5f$ character give rise to the NEXAFS spectra presented in Fig. 5. These data were obtained using the total-electron-yield method; the spectra are characterized by intense white lines due to $3d$-$5f$ optical transitions and by rather weak edge profiles. In this respect, they resemble the well-known $M_{4,5}$ spectra of the RE compounds.[19–22] The white lines, however, do not

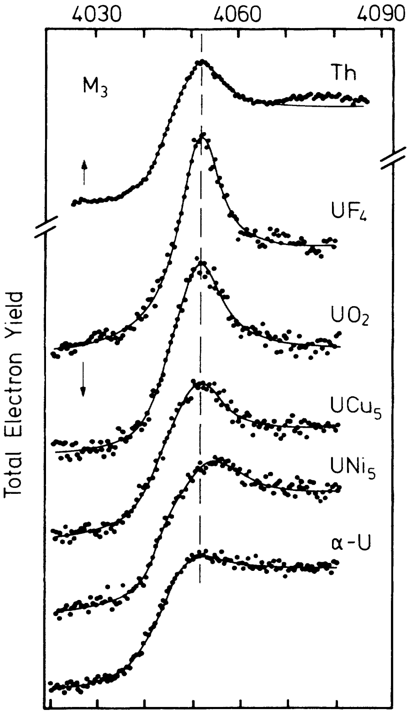

FIG. 4. Total-electron-yield spectra of various U compounds (and of Th metal for comparison) at the M_3 threshold. The solid lines represent fit results.

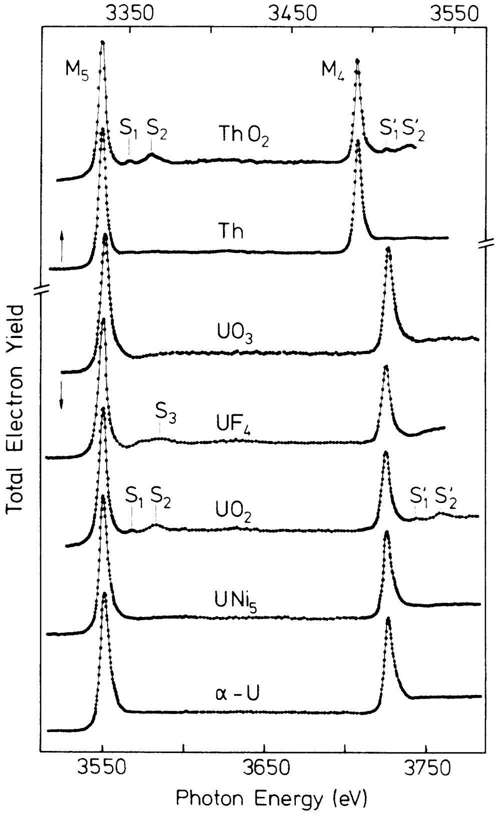

FIG. 5. Total-electron-yield spectra of various U and Th systems at the $M_{4,5}$ thresholds. The solid lines serve as guides to the eye. S_1, S_2, and S_3 as well as the dotted symbols denote NEXAFS peaks due to multiple-scattering resonances (see text).

exhibit any resolved multiplet splitting from the $3d^95f^{n+1}$ exchange interaction; rather, they look quite similar for such different systems as α-U metal (delocalized $5f$) and UO_2 or UF_4 (localized $5f$).

Some of the spectra in Fig. 5 exhibit additional peaks at energies up to 40 eV above threshold. These structures are particularly visible in the spectra of ThO_2, UO_2, and UF_4; they are designated in Fig. 5 by S_1, S_2, and S_3 (above M_5) and the corresponding primed symbols (above M_4). The structures look identical above the two thresholds. We assign these NEXAFS features to MS resonances, which contain information on the local structure around the absorbing central atom. The energetic positions of these MS resonances above the white-line maxima are $\simeq$17 eV (31 eV) for S_1 and S_1' (S_2 and S_2') in ThO_2 and UO_2, and $\simeq$38 eV for S_3 in UF_4.

One would first expect these MS resonances to be strong in crystal structures with highly coordinated and well-separated nearest-neighbor (NN) and next-nearest-neighbor (NNN) shells. This is supported by the pronounced MS peaks observed for ThO_2 and UO_2, which both crystallize in the CaF_2 structure with an An—O bond length of 2.42 Å (2.37 Å) and an An—An distance of 3.95 Å (3.87 Å) in the case of ThO_2 (UO_2); on the other hand,,no MS resonances are visible in the $M_{4,5}$ spectra of Th metal, which also crystallizes in a highly coordinated (fcc) structure. It therefore seems that the appearance of these MS peaks is particularly favored in nonmetallic systems with covalent metal-ligand bonds like, e.g., the An—O bond.

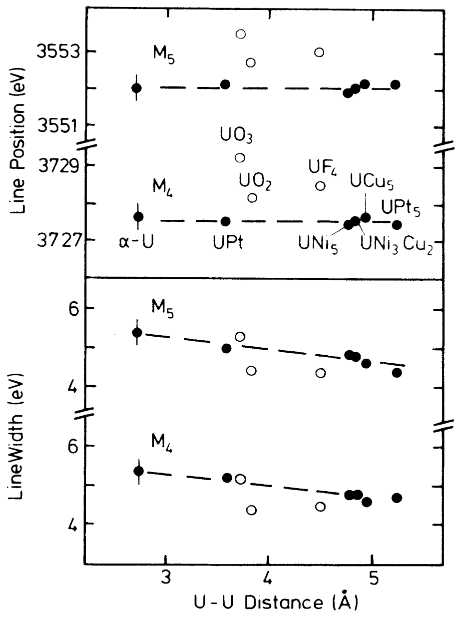

FIG. 6. Line positions and linewidths of the $M_{4,5}$ white-line peaks of various U compounds, plotted versus the nearest-neighbor U—U distance. The error bars given represent absolute errors, while the relative errors are smaller than the dimensions of the data points.

The $M_{4,5}$ spectra were fitted to a superposition of an asymmetric Lorentzian[38] and an arctangent function; this spectral shape was convoluted with the experimentally determined rocking curve, which was analytically described by a superposition of Gaussian and asymmetric Lorentzian line shapes (Voigt line). The resulting positions and deconvoluted widths of the white lines are plotted in Fig. 6 as a function of the U—U distance. In this figure, the nonmetallic compounds UF_4, UO_3, and UO_2 are distinguished by open circles from the metallic compounds, which are represented by solid circles.

We infer from Fig. 6 that the positions of the white lines are practically identical (within experimental accuracy) for all metallic compounds studied, while they are shifted to higher energy for the insulating compounds, up to $\simeq$1.5 eV (for UO_3). The linewidths observed for the metallic systems decrease by about 1 eV (corresponding to $\simeq$20%) with increasing NN U—U distance, approaching the value found for the nonmetallic compounds UO_2 and UF_4. Compared to the Th compounds investigated, the $M_{4,5}$ white lines of the U compounds are about 20% broader. Furthermore, an asymmetric broadening to higher energy is observed for the white lines, particularly in the case of the metallic compounds and UO_3.

The widths of the white lines are determined by the lifetime width of the core hole, a possible broadening due to $3d^95f^{n+1}$ exchange interaction, and a contribution from the bandwidth of the empty $5f$ states. For Th, an estimate for the lifetime widths is available from atomic calculations: 2.9 eV for M_5 and 3.2 eV for M_4.[41] These values are in good agreement with our experimental results (3.5 eV at both edges). It should be noted that multiplet-splitting effects are not expected to contribute to the Th $M_{4,5}$ linewidths, since the $M_{4,5}$ multiplet spectra are dominated by one intense single line each with only weak satellites (similar to the $3d^94f^1$ spectrum of La). For U, an $M_{4,5}$ linewidth of $\simeq$3.5 eV may be estimated,[41] which is about 1 eV smaller than our experimental results.

An estimate for the contribution of the $3d^95f^{n+1}$ exchange interaction can be made from recent atomic calculations by Sawatzky.[42] For a $3d^95f^3$ configuration (corresponding to UO_2 and UF_4), this author found a total width of the $M_{4,5}$ multiplet of $\simeq$2.5 eV; splittings of similar size were also obtained for the $3d^95f^4$ configuration. When these theoretical multiplet structures are convoluted with Lorentzian lines of $\simeq$3 eV (FWHM) for lifetime broadening as well as with the experimental rocking curve, essentially single lines with no resolved multiplet structure are obtained, in agreement with our observations.

The variation of the $M_{4,5}$ linewidths with U—U distance (see Fig. 6) seems to be correlated with the bandwidth of the unoccupied $5f$ states. A possible contribution from the $3d^95f^{n+1}$ multiplet splitting would be expected to show just the opposite behavior, since the increase in $5f$ localization at larger U-U distances should lead to increased Coulomb and exchange interactions. In the same direction, however, the $5f$ bandwidth is expected to decrease, in accordance with the observed decrease in the $M_{4,5}$ linewidths. The linewidths determined in this work compare favorably with previous results for UAl_2,

UMn_2, and USn_3,[14] but are considerably narrower than obtained before for α-U metal and UO_2.[10]

A line-shape analysis of the $M_{4,5}$ peaks reveals substantial asymmetries to higher energy, particularly in the case of the metallic systems and UO_3. The asymmetry of the lines is measured by the ratio α of the half width at half maximum of an asymmetric Lorentzian fitted to the peaks.[38] The resulting values of α range from 1.2 to 1.5 for the M_5 peaks and from 1.3 to 1.7 for the M_4 peaks. These line asymmetries do not scale with the total linewidths of the $M_{4,5}$ peaks plotted in Fig. 6. Several mechanisms may contribute to these asymmetries: (i) Multielectron excitations due to the creation of a core hole,[43] as well as unresolved satellite features due to excitations of the $5f$ electron system, analogous to the RE case.[19,20,25] (ii) Transitions into unoccupied valence-band states with f symmetry above the ionization threshold, which would be possible due to hybridization of $5f$ states with valence orbitals.[16]

Also extracted from the spectra of Fig. 5 were the relative amplitudes r of the white-line peaks with respect to the edge jumps. For the U systems the fit results for r range from 8—9 at M_5 and from 6—7 at M_4, and show no dependence on the metallic or insulating nature of the compounds. These numbers are considerably larger than previously reported for the $M_{4,5}$ spectra of several intermetallic U compounds, where values close to 3 were observed.[14] Similar r values may also be deduced from the spectra of α-U metal and UO_2 given in Ref. 10. These previous $M_{4,5}$ spectra were measured in transmission geometry using thin absorbers, while the present spectra given in Fig. 5 were obtained by the total-electron-yield method. We therefore checked our results for a possible influence of the different detection modes. For this purpose, absorption measurements were also performed on UF_4 and UO_2, using thin homogeneous absorbers prepared by dispersing finely powdered compounds in methanol onto filter paper. The resulting XA spectra were found to be practically identical to the total-electron-yield spectra of Fig. 5, resulting in the same ratios r. This supports our assumption that the total-electron-yield method gives essentially the correct XA line shapes. The deviations of the previously reported $M_{4,5}$ spectra from our present results may have been caused by saturation effects due to thick or inhomogeneous absorbers or even by nonlinearities in the photographic film material employed in the earlier work.

In view of the present $M_{4,5}$ spectra for a large variety of U compounds with rather different $5f$ electronic structures, the previously reported M_5 data for Pu metal in the region of the α-to-δ phase transition are quite remarkable.[11] In δ-Pu metal, a single M_5 peak with a vanishing edge jump was reported, while for α-Pu metal, a splitting of the main peak with two additional weak satellites was observed. The data were interpreted in support of an increased $5f$ localization in δ-Pu metal. This would mean that comparably large changes in the electronic nature of the $5f$ states are totally absent in the U compounds studied. In view of recent theoretical results, indicating that $5f$ localization is not expected in actinides lighter than Pu,[44] as well as previous arguments on extended $5f$ states in UO_2,[45] such a conclusion would seem reasonable.

VI. SOFT-XA SPECTRA AT THE $N_{4,5}$ THRESHOLDS

We have also studied the soft-XA spectra of α-U metal, UF_4, and ThO_2 (for comparison) at the $N_{4,5}$ thresholds by the total-electron-yield method. The results for UF_4 and α-U metal are presented in Fig. 7; they were obtained at BESSY using the SX-700 monochromator at a resolution of 1.4 eV (FWHM). The spectra are characterized by intense NEXAFS peaks due to $4d$-$5f$ transitions (separated by the $4d$ spin-orbit splitting) and undetectably weak edge jumps. The higher white-line intensity relative to the edge jump as compared to the $M_{4,5}$ spectra is, in fact, expected from the increased $4d$-$5f$ orbital overlap, leading to higher transition rates into the $5f$ states. It also explains the absence of observable MS peaks above the white lines as observed in the $M_{4,5}$ spectra (see above).

The $N_{4,5}$ spectra in Fig. 7 clearly show no resolved multiplet splitting from the $4d^95f^{n+1}$ exchange interaction, which is expected to be larger than in the $M_{4,5}$ spectra due to the increased orbital overlap. The peaks are well described by symmetric Lorentzian lines with the exception of the N_4 peak of α-U metal, where a line shape slightly asymmetric towards higher energies ($\alpha \simeq 1.3$) had to be assumed. The fit results (solid lines in Fig. 7) show a small (0.5 eV) shift to higher energies for the $N_{4,5}$ peaks of UF_4 relative to α-U metal, in agreement with the findings from the $M_{4,5}$ spectra. Also, the N_5 peak of α-U metal is wider than that of UF_4 (6.9 versus 5.5 eV), while the N_4 peaks of both U systems have very similar widths (6.0 versus 5.9 eV). The latter minor difference from the $M_{4,5}$ spectra could indicate contributions to the $N_{4,5}$ linewidths from the $4d^95f^{n+1}$ multiplet splitting in addition to contributions from the lifetime widths of the $4d$ core holes (calculated to be $\simeq 4$ eV for an N_5 core hole),[41] as well as from the bandwidth of the unoccupied $5f$ states. The $N_{4,5}$ peaks of both U systems are wider than those of ThO_2 (4.5 eV), again in agreement with the $M_{4,5}$

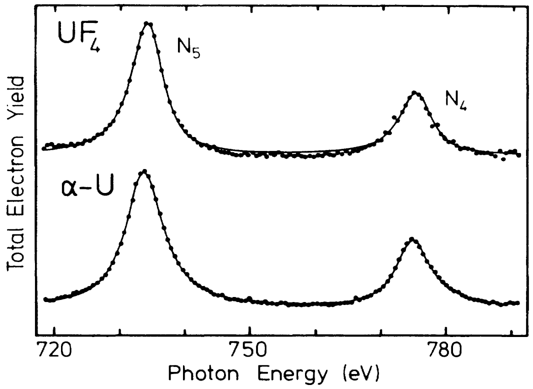

FIG. 7. Total-electron-yield spectra of α-U metal and UF_4 at the $N_{4,5}$ thresholds. The solid lines represent fit results.

results (see Fig. 6).

In both U systems studied, the ratio of intensity of the absorption peak at N_5 relative to that at N_4 is found to be 2.1, which may be compared with a ratio of 1.7 observed in the $M_{4,5}$ spectra and the statistical value of 1.5 from the degeneracy of the $d_{5/2}$ and $d_{3/2}$ hole states. Since the latter value is only expected in the absence of electron correlations, the observed trend is plausible in view of the expected increase in core-hole—$5f$ interaction due to the increase in orbital overlap from $3d$ to $4d$.

VII. SOFT-XA SPECTRA AT THE $O_{4,5}$ THRESHOLDS

A further increase in the orbital overlap between core-hole and $5f$ electrons, resulting in strong multiplet effects, is found in the soft-XA spectra at the $O_{4,5}$ thresholds. In this case, the $5d$-$5f$ exchange interaction is of the same order of magnitude as the $5d^9$ spin-orbit interaction. The $O_{4,5}$ spectra are therefore similar to the $4d^9 4f^{n+1}$ excitation spectra in RE systems, which have been studied extensively, both theoretically and experimentally.[23,30] The question arises as to whether the $O_{4,5}$ spectra of U and Th systems can be interpreted in a similar atomiclike way as $5d^9 5f^{n+1}$ final-state multiplets, despite the less localized character of the $5f$ states. Up to now, only few and partly controversial experimental results have been reported on Th and α-U metal,[46,47] as well as on UF_4 in the vapor phase.[13]

We have therefore studied the $O_{4,5}$ spectra of ThF_4 and of various U compounds in the total-electron-yield mode, using the SX-700 beam line at BESSY with an instrumental resolution of $\simeq$100 meV. Representative spectra are presented in Fig. 8; note the different energy scales for the ThF_4 and the U spectra.

The ThF_4 spectrum consists of two strong peaks (P_1,P_2) and a very weak peak (P_3), in good agreement with the multiplet structure obtained from intermediate-coupling calculations for an atomiclike $5d^9 5f^1$ final-state configuration.[46] It is actually quite similar to the $N_{4,5}$ spectra of LaF_3 and CeF_4, which are known to be caused by $4d^9 4f^1$ final states due to the empty localized $4f$ ground states.[23] The atomiclike $O_{4,5}$ spectrum of ThF_4 therefore indicates a rather localized $5f^1$ excited state, probably due to the influence of the final-state core hole.[46]

The $O_{4,5}$ spectrum of solid UF_4 given in Fig. 8 agrees well with a previously published result for UF_4 in the vapor phase.[13] At least four peaks (denoted by A, B, C, and D) can be identified in this spectrum. They are well explained by the results of a recent multiplet calculation by Sawatzky for atomiclike $5d^9 5f^3$ excitations.[42] At least in the final state with a $5d$ core hole, UF_4 is therefore characterized by rather localized $5f$ electrons; the spectrum suggests a $5f^2$ ground state.

The $O_{4,5}$ spectra of the metallic U systems studied in this work exhibit much broader peaks, particularly in α-U metal. A similar broadening and loss of multiplet features has previously been observed in the $4d$-$4f$ excitation spectra of Ce compounds.[23] It is consistent with the more itinerant $5f$ character and strong conduction electron hybridization in metallic U compounds as compared to UF_4. Peaks B and C can be clearly identified in the UCu_5 spectrum, but are practically absent in the spectra of UNi_5 and α-U metal, indicating an increase in $5f$ delocalization. The differences in the spectra of UCu_5 and UNi_5 are in agreement with the conclusions of a recent PE-BIS study of the UCu_xNi_{5-x} system, which showed an increase in $5f$ localization with increasing x. In addition to this loss of multiplet structure, the main peak in the $O_{4,5}$ spectrum of the metallic systems (F) is shifted by $\simeq$1.5 eV to higher energy as compared to UF_4.

The spectrum of α-U metal in the present work agrees well with the results of Moser *et al.* obtained by the electron-energy-loss spectroscopy (EELS) method,[46] as well as with the earlier work of Cukier *et al.* by XA and EELS.[47] However, it disagrees strongly with observations of Connerade *et al.*,[13] who claimed a close similarity of the spectra of α-U metal and of UF_4 in the vapor phase. These measurements were performed in transmission geometry and the metal data were obtained from eva-

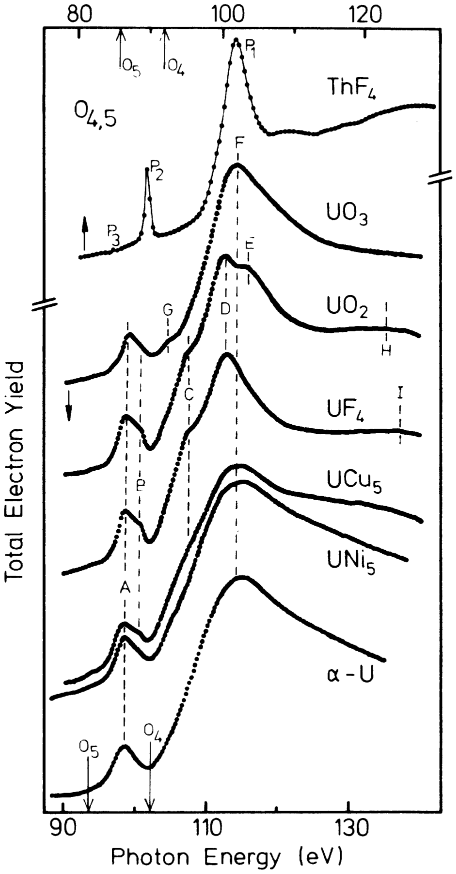

FIG. 8. Total-electron-yield spectra of various U compounds and of ThF_4 at the $O_{4,5}$ thresholds. Note the different energy scales for the Th and U spectra; the arrows specify the O_4 and O_5 thresholds from XPS measurements of Th and α-U metal, respectively (Ref. 46). The various spectral features are explained in the text. The solid lines through the data points serve as guides to the eye.

porated thin U films; we suspect that the results may have been influenced by oxygen contamination.

The $5f$ character in UO_2 is known to be rather localized; therefore similar $O_{4,5}$ spectra are expected for UO_2 and UF_4. Indeed, the two spectra, given in Fig. 8, differ only by the additional peak E observed in the UO_2 spectrum at $\simeq 116$ eV. This feature is about 15 eV above the O_5 threshold from x-ray photoemission spectroscopy (XPS) measurements[46] and therefore could well be caused by a MS NEXAFS resonance as discussed above in connection with the $M_{4,5}$ spectra. In fact, the S_1 and S_1' satellites observed in the $M_{4,5}$ spectrum of UO_2 (Fig. 5) were found at $\simeq 17$ eV higher energies than the main M_5 and M_4 resonance lines, respectively. An indication for a MS peak corresponding to the S_2 and S_2' peaks in the $M_{4,5}$ spectra of UO_2 is also given by feature H in Fig. 8; this peak, however, is rather broad and therefore less visible. In the case of UF_4, a broad feature (S_3) due to multiple scattering has been identified at an energy of $\simeq 34$ eV above the main M_5 peak (see Fig. 5), which would imply a broad feature around position I in the $O_{4,5}$ spectrum of UF_4. This is fully consistent with the present observation, and the differences in the $O_{4,5}$ spectra of UF_4 and UO_2 are thus explained as being due to different MS NEXAFS resonances related to the local structural environment.

Figure 8 also shows the $O_{4,5}$ spectrum obtained for UO_3; it is totally different from the spectrum of the $5f^0$-system ThF_4 and clearly shows that the formally hexavalent UO_3 is characterized by a substantial $5f$ count in the ground state. This is in agreement with the results of calculations via the multiple-scattering X_α method for UF_6 by Boring and Wood[35] where a $5f$ charge between 2.3 and 3.4 was found within the atomic sphere of U. These $5f$ states are strongly hybridized with O $2p$ ligand orbitals, causing the broad features in the $O_{4,5}$ spectrum of UO_3 and little resolved multiplet structure. The spectrum therefore looks very similar to those observed for the metallic U systems. The weak peak G at $\simeq 105$ eV is not observed in any of the other U systems studied. Note that the analogy with the MS NEXAFS peaks in $M_{4,5}$ and $O_{4,5}$ spectra may be carried even further. No such features were observed in the $M_{4,5}$ spectra of UO_3, UNi_5, and α-U metal, in agreement with their absence in the corresponding $O_{4,5}$ spectra given in Fig. 8.

VIII. SUMMARY AND CONCLUSIONS

The results of the present study show that NEXAFS spectra at the L_3 and M_3 thresholds of U compounds contain valuable information on the unoccupied $6d$ density of states. This is clearly borne out in the appreciable variations in width and relative intensity of the white line, particularly in the metallic systems. The sensitivity of the energetic position of the white line to $5f$ occupancy is displayed by the observed 4-eV shift between UCl_3 and the formally tetravalent compounds UF_4 and UO_2. In UO_3, however, the position of the white line shows that only minor changes in $5f$ occupancy occur when proceeding from a formally tetravalent to a hexavalent U compound, in agreement with theoretical results. In the metallic systems studied, the white-line positions display only minor variations.

The NEXAFS spectra at the $M_{4,5}$ and $N_{4,5}$ thresholds are dominated by white-line peaks from optical transitions into unoccupied $5f$ states. At the $M_{4,5}$ threshold, they may be measured both by absorption and total-electron-yield techniques. The intense white lines show no resolved multiplet structure, in agreement with theoretical estimates, but their widths vary in metallic systems with the U—U distance, suggesting a correlation with the $5f$ bandwidth.

At the $O_{4,5}$ thresholds in the soft-x-ray region, NEXAFS spectra with well-resolved structures are observed which can be quantitatively described by spin-orbit and exchange interactions of similar size in the $5d^9 5f^{n+1}$ final state. In the nonmetallic compounds, like UF_4 and UO_2, these spectra are atomiclike, while the structures are much broader in the metallic systems and almost totally washed out in α-U metal. This is quite similar to previous observations in the $M_{4,5}$ and $N_{4,5}$ NEXAFS spectra of Ce compounds.

In the $M_{4,5}$ and $O_{4,5}$ spectra of several nonmetallic Th and U compounds, additional peaks at energies between 15 and 38 eV above threshold are observed, which are interpreted as multiple-scattering resonances. These peaks are particularly visible in the spectra of UO_2 and ThO_2. It is shown that these MS peaks appear also in the $O_{4,5}$ spectra, an observation which greatly facilitates the interpretation of the rather complicated structure of the $O_{4,5}$ NEXAFS spectra, e.g., of UO_2.[48]

The present work shows that XA studies at the L_3 and $M_{4,5}$ thresholds are very promising for electronic-structure studies of the light actinide elements Np, Pu, and Am as well as their compounds. Particularly at the L thresholds, encapsulated samples may be studied, avoiding totally the experimental safety problems connected with the radioactivity of these elements. Work in this direction is in progress.

ACKNOWLEDGMENTS

We wish to thank Professor B. Kanellakopulos for providing us with the UCl_3 sample, as well as Professor G. A. Sawatzky for stimulating discussions and for making available to us the results of his core-hole—$5f$-multiplet calculations prior to publication. For assistance and support during various parts of the measurements, we thank Dr. C. Laubschat, Dr. M. Domke, Dr. E. Paparazzo, and A. Schach von Wittenau. The hospitality of Professor D. A. Shirley, Lawrence Berkeley Laboratory, during the experiments at SSRL, and the cooperation of the staffs at DESY, Hamburg; BESSY, Berlin; and SSRL, Stanford are gratefully acknowledged. This work was supported by the Bundesminister für Forschung und Technologie, project No. 05 313AX B2, TP4.

[1] *Actinides-Chemistry and Physical Properties,* edited by L. Manes (Springer-Verlag, New York, 1985).

[2] M. S. S. Brooks, B. Johansson, and H. L. Skriver, in *Handbook on the Physics and Chemistry of the Actinides,* edited by A. J. Freeman and G. H. Lander (North-Holland, Amsterdam, 1984).

[3] Y. Baer and J. K. Lang, Phys. Rev. B **21**, 2060 (1980).

[4] Y. Baer, H. R. Ott, and K. Andres, Solid State Commun. **36**, 387 (1980).

[5] B. Reihl, N. Mårtensson, P. Heimann, D. E. Eastman, and O. Vogt, Phys. Rev. Lett. **46**, 1480 (1981).

[6] Y. Baer and J. Schoenes, Solid State Commun. **33**, 885 (1980).

[7] M. Brown, R. E. Peierls and E. A. Stern, Phys. Rev. B **15**, 738 (1977).

[8] P. H. Citrin, G. K. Wertheim, and M. Schlüter, Phys. Rev. B **20**, 3067 (1979).

[9] G. van der Laan, J. Zaanen, G. A. Sawatzky, R. Karnatak, and J. M. Esteva, Phys. Rev. B **33**, 4253 (1986).

[10] Y. Cauchois, C. Bonnelle, and I. Manescu, C. R. Acad. Sci. Ser. B **267**, 817 (1968); C. Bonnelle and G. Lachere, J. Phys. (Paris) **35**, 295 (1974).

[11] C. Bonnelle, A. Courtois, and D. Calais, in *Plutonium and Other Actinides,* edited by H. Blank and R. Lindner (North-Holland, Amsterdam, 1976), p. 343.

[12] C. Bonnelle, Struct. Bonding (Berlin) **31**, 23 (1976).

[13] J. P. Connerade, M. W. D. Mansfield, M. Cukier, and M. Pantelouris, J. Phys. B **13**, L235 (1980).

[14] J. M. Lawrence, M. L. den Boer, R. D. Parks, and J. L. Smith, Phys. Rev. B **29**, 568 (1984).

[15] D. H. Templeton and L. K. Templeton, Acta Crystallogr. Sect. A **38**, 62 (1982).

[16] J. Petiau, G. Calas, D. Petitmaire, A. Bianconi, M. Benfatto, and A. Marcelli, Phys. Rev. B **34**, 7350 (1986).

[17] M. Benfatto *et al.*, Solid State Commun. **46**, 367 (1983).

[18] G. Materlik, J. E. Müller, and J. W. Wilkins, Phys. Rev. Lett. **50**, 267 (1983).

[19] J. C. Fuggle, F. U. Hillebrecht, J. M. Esteva, R. C. Karnatak, O. Gunnarsson, and K. Schönhammer, Phys. Rev. B **27**, 4637 (1983).

[20] G. Kaindl, W. D. Brewer, G. Kalkowski, and F. Holtzberg, Phys. Rev. Lett. **51**, 2056 (1983); G. Kaindl, G. Kalkowski, W. D. Brewer, E. V. Sampathkumaran, F. Holtzberg, and A. Schach von Wittenau, J. Magn. Magn. Mater. **41&42**, 181 (1985); W. D. Brewer, G. Kalkowski, G. Kaindl, and F. Holtzberg, Phys. Rev. B **32**, 3676 (1985).

[21] J. Sugar, W. D. Brewer, G. Kalkowski, G. Kaindl, and E. Paparazzo, Phys. Rev. A **32**, 2242 (1985).

[22] B. T. Thole, G. van der Laan, J. C. Fuggle, G. A. Sawatzky, R. C. Karnatak, and J. M. Esteva, Phys. Rev. B **32**, 5107 (1985).

[23] G. Kalkowski, C. Laubschat, W. D. Brewer, E. V. Sampathkumaran, M. Domke, and G. Kaindl, Phys. Rev. B **32**, 2717 (1985).

[24] E. V. Sampathkumaran, G. Kaindl, W. Krone, B. Perscheid, and R. Vijayaraghavan, Phys. Rev. Lett. **54**, 1067 (1985).

[25] O. Gunnarsson and K. Schönhammer, Phys. Rev. B **28**, 4315 (1983).

[26] T. Jo and A. Kotani, Solid State Commun. **54**, 451 (1985).

[27] See, e.g., J. Haase, Appl. Phys. A **38**, 181 (1985), and references therein.

[28] P. M. De Wolff, Acta Crystallogr. **14**, 322 (1961).

[29] A. F. Starace, Phys. Rev. B **5**, 1773 (1972).

[30] J. Sugar, Phys. Rev. B **5**, 1785 (1972).

[31] See, e.g., *Proceedings of the 4th International Conference on Valence Fluctuations,* edited by E. Müller-Hartmann, B. Roden, and D. Wohlleben (North-Holland, Amsterdam, 1985).

[32] H. J. van Daal, K. H. J. Buschow, P. B. van Aken, and M. H. van Maaren, Phys. Rev. Lett. **34**, 1457 (1975).

[33] F. U. Hillebrecht, D. D. Sarma, and N. Mårtensson, Phys. Rev. B **33**, 4376 (1986).

[34] R. D. Parks, S. Raaen, M. L. den Boer, and V. Murgai, Phys. Rev. B **28**, 3556 (1983).

[35] M. Boring and J. H. Wood, J. Chem. Phys. **71**, 32 (1979).

[36] E. A. Stern, Phys. Rev. Lett. **49**, 1353 (1982).

[37] J. J. Pireaux, J. Riga, E. Thibaut, C. Tenret-Noel, R. Caudano, and J. J. Verbist, Chem. Phys. **22**, 113 (1977).

[38] For the asymmetric Lorentzian line shape, two Lorentzians with different half widths at half maximum were joined continuously at their respective maxima. The asymmetry parameter α of the resulting line shape is given by the ratio of the half width at half maximum at higher energy to that at lower energy.

[39] B. W. Veal, D. J. Lam, W. T. Carnall, and H. R. Hoeckstra, Phys. Rev. B **12**, 5651 (1975).

[40] L. G. Parrat, C. F. Hempsteadt, and E. L. Jossen, Phys. Rev. **105**, 1228 (1957); E. A. Stern and K. Kim, Phys. Rev. B **23**, 3781 (1981).

[41] O. M. Krause, J. Phys. Chem. Ref. Data **8**, 307 (1979); O. Keski-Rahkonen and O. M. Krause, At. Data Nucl. Data Tables **14**, 139 (1974), and references therein.

[42] G. A. Sawatzky (private communication).

[43] See, e.g., U. Fano, Phys. Rev. **124**, 1866 (1961); P. Nozieres and C. T. De Dominicis, *ibid.* **178**, 1097 (1969); S. Doniach and M. Sunic, J. Phys. C **3**, 285 (1970).

[44] W. A. Harrison, Phys. Rev. B **29**, 2917 (1984).

[45] L. E. Cox, J. Electron Spectrosc. Relat. Phenom. **26**, 167 (1982); M. S. S. Brooks and P. J. Kelly, Solid State Commun. **45**, 689 (1983).

[46] H. R. Moser, B. Delley, W. D. Schneider, and Y. Baer, Phys. Rev. B **29**, 2947 (1984).

[47] M. Cukier, P. Dhez, B. Gauthe, P. Jaegle, Cl. Wehenkel, and F. Combet Farnoux, J. Phys. (Paris) Lett. **39**, L315 (1978).

[48] G. Kaindl *et al.* (unpublished).